International Journal of Earth Sciences (2018) 107:2999–3004
https://doi.org/10.1007/s00531-018-1634-6

SHORT NOTE

A first-order model for temperature rise for uniform and differential compression of sediments in basins

Soumyajit Mukherjee[1] · **Nishant Kumar**[1]

Received: 3 May 2018 / Accepted: 8 July 2018 / Published online: 16 July 2018

Abstract
We deduce algebraic expressions for temperature rise for ideal cases of uniform and spatially varying compression of sediments of single mineralogy. According to the results of the present work, the temperature rise is related to the coefficient of volume expansion, isothermal compressibility, dimension, bulk density, and specific heat of the sediment columns. Rise of temperature due to compression of sediment is effectively inversely proportional to the volume coefficient of expansion (or contraction) of sediments. Compression-related temperature rise is expected to augment diagenesis. A more realistic model of temperature rise dealing with the rate of compression of sediments that of the pore fluid(s) and the vacant pore space individually would be required.

Keywords Sediment compaction · Compression · Basin evolution · Thermal structure

Introduction

Mechanical compaction of clastic sediments with coevally falling void ratios associated with porosity reduction is related to effective stress, which is the overburden stress minus the pore fluid pressure (Bjorlykke 1999), and sometimes, the magnitude is taken as a direct measure of compaction (Hantschel and Kauerauf 2008). Compacting sediments, especially mudstones (Bjorlykke 1999), and certain muddy stones (Worden and Burley 2003) behave ductilely and hence their compaction can be compared with that of fluid under compression, so long sediments do not fracture. For clay layers, a depthwise pressure gradient of 10^4 Pa m^{-1} can develop (Wangen 2010).

Conversion of shale from mud can be due to overburden pressure (Cloetingh and Ziegler 2007). Usually, sediments with finer grains compact more efficiently (Pettijohn 2004), since they consist of high volume of clay that usually retains high water as clay bound water. For example, mud layers with 10^{-6} Pa^{-1} of compressibility (Payne et al. 2008) can shrink up to one-tenth of their original widths (Tucker 1981). The other magnitudes of compressibility of argillaceous sediments can be found in Rieke and Chilingarian (1974). Likewise, peat-to-coal conversion can reduce thickness of the original peat layer by a factor of 11 (Ryer and Langer 1980). For unconsolidated materials, the compaction constant [λ in Athy's equation, where $p_z = p_s e^{-(z/\lambda)}$; p_s porosity at surface; p_z that at depth z] can vary from 1.0 (completely compacted sediment) up to ~ < 1.6 (undercompacted variety). Sediments can be buried up to several km depth (Nemec 1988), which means that mud with bulk density 1.8 gm cm^{-3} (Murton and Biggs 2003) can be below $\sim 5.8 \times 10^{10}$ Dyne cm^{-2} of pressure (as per the formula: pressure = density × acceleration due to gravity × depth). Compression has been linked with change in porosity as follows (Blatt et al. 1972):

$$S = H(\Phi_0 - \Phi)(1 - \Phi)^{-1}, \quad (1)$$

where H thickness of sedimentary layer, Φ_0 initial porosity, and Φ final porosity. Note here, "$1-\Phi$" means the volume of solids divided by the total volume of the rock.

The thermal data so far have not been considered in studies of sediment compaction and compression-related heat. This work models vertical compression-related temperature rise in sedimentary basins. Adding model-derived compression-related temperature rise into the thermal structure/anomaly of the basin would be the next useful exercise. Temperature structure matters for petroliferous basins, since

✉ Soumyajit Mukherjee
soumyajitm@gmail.com

[1] Department of Earth Sciences, Indian Institute of Technology Bombay, Powai, Mumbai, Maharashtra, India

that can affect thermal maturation of source rocks (Blackwell and Steele 1989). Positive geothermal anomalies have been reported from some overpressured zones (L'heureux and Fowler 2000), where shales can get over-compacted (Chilingarianet al. 1995).

The model

Uniform compression throughout the basin

Basins can be subsiding uniformly (Weeks 1952) especially if they are symmetric and devoid of any growth strata, or they can do so at least during part of their depositional history (Wood 1981). Here, we consider a simple and ideal case of a rigid basement over which sediments undergo compression due to load of its overburden. Consider a rectangle ABCD with a compressible fluid inside it (Fig. 1a). Uniaxial compression is considered (as per Fjaret al. 2008), whereby AB moves towards CD with a constant velocity 'v'.

Temperature change (dT) can be expressed as

$$\mathrm{d}T = (\partial T/\partial V)_P \mathrm{d}V + (\partial T/\partial P)_V \mathrm{d}P, \tag{2}$$

where V volume, P pressure, and T temperature of the fluid. Subscripts in Eqs. (2) to (6) and (9) indicate that those are constants.

Now, coefficient of volume expansion:

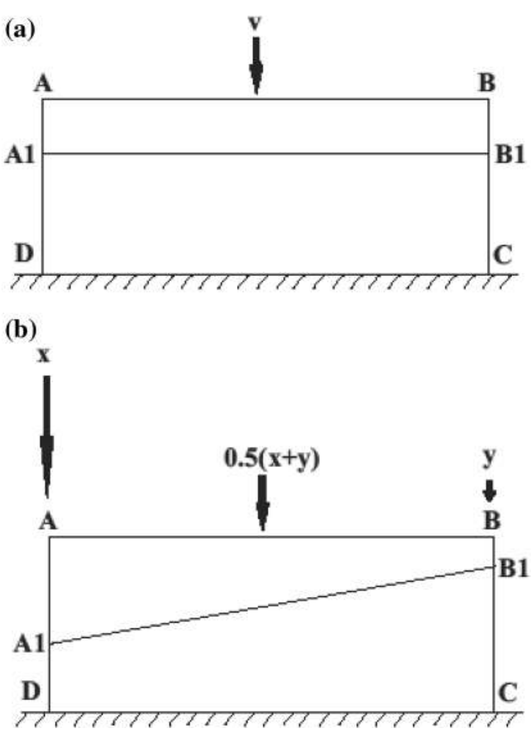

Fig. 1 Compression of sedimentary layer. AB length$=l_0$; AD$=h_0$; **a** uniformly, **b** non-uniformly

$$\beta = (\partial V/\partial T)_P V^{-1}. \tag{3}$$

In addition, isothermal compressibility:

$$k = -(\partial V/\partial P)_T V^{-1}. \tag{4}$$

Considering a constant compressibility of rocks is justified, since it does not change (much) during compaction (Hantschel and Kauerauf 2008). An important relation amongst differentials:

$$(\partial P/\partial T)_V \times (\partial T/\partial V)_P \times (\partial V/\partial P)_T = -1. \tag{5}$$

Using Eqs. (2)–(5)

$$\mathrm{d}T = \beta^{-1}V^{-1}\mathrm{d}V - \left\{(\partial T/\partial V)_{P*}(\partial V/\partial P)_T\right\}\mathrm{d}P. \tag{6}$$

Or

$$\mathrm{d}T = \beta^{-1}V^{-1}\mathrm{d}V + k\beta^{-1}\mathrm{d}P. \tag{7}$$

Recall the thermodynamic relation:

$$\mathrm{d}H = \mathrm{d}U + P\mathrm{d}V + V\mathrm{d}P. \tag{8}$$

H and U are enthalpy heat and internal energy, respectively.

Presuming no heat is lost from the body into the surrounding

$$nC_\mathrm{p}\mathrm{d}T = V\mathrm{d}P, \tag{9}$$

where n kg per moles in the body and C_p specific heat at constant pressure. The consideration of C_p is justified, since the model considers constant applied pressure.

Eliminating dP from Eqs. (7) and (9):

$$\mathrm{d}T = \beta^{-1}V^{-1}\left[\mathrm{d}V + knC_\mathrm{p}\mathrm{d}T\right], \tag{10}$$

$$\mathrm{d}T = \mathrm{d}V\left\{V\beta - knC_\mathrm{p}\right\}^{-1}, \tag{11}$$

Or

$$\int_{T_0}^{T} \mathrm{d}T = \int_{V_0}^{V} \mathrm{d}V\left\{V\beta - knC_\mathrm{p}\right\}^{-1}. \tag{12}$$

This yields

$$T = T_0 + \beta^{-1}\ln\left\{\left(V\beta - knC_\mathrm{p}\right)\left(V_0\beta - knC_\mathrm{p}\right)^{-1}\right\}. \tag{13}$$

The initial geometric dimensions of the sedimentary package are $l_{0,}$ $b_{0,}$ and h_0, and after time 't', h changes to (h_0−vt), respectively. Therefore

$$V = V_0 - l_0 b_0 vt. \tag{14}$$

Eliminating 'V' from Eqs. (13) and (14),

$$\Delta T = T - T_0 = \beta^{-1}\ln\left\{(1 - \beta l_0 b_0 vt\left(V_0\beta - knC_\mathrm{p}\right)^{-1}\right\}. \tag{15}$$

The relation amongst molar mass ratio (r), mass (m), and moles (n) is

$$r = n m^{-1}. \tag{16}$$

Eliminating 'n' from Eqs. (15) and (16)

$$\Delta T_1 = T - T_0 = \beta^{-1} \ln \left\{ (1 - \beta l_0 b_0 v t \left(V_0 \beta - krmC_p \right)^{-1} \right\}. \tag{17}$$

Now

$$m = V_0 \rho. \tag{18}$$

Therefore

$$\Delta T_1 = \beta^{-1} \ln \left\{ 1 - \beta l_0 b_0 v t V_0^{-1} (\beta - kr\rho C_p)^{-1} \right\}. \tag{19}$$

Since we consider volumetric contraction, 'β' inside second bracket should be opposite in sign than what is represented for volumetric expansion. Second, magnitude of compressibility contains inherently a negative sign (see Eq. 4). Therefore, its sign needs to be reversed to utilize its absolute magnitude. The final working equation thus becomes

$$\Delta T_1 = \beta^{-1} \ln \left\{ 1 + \beta l_0 b_0 v t V_0^{-1} (kr\rho C_p - \beta)^{-1} \right\}. \tag{20}$$

Spatially non-uniform/differential compression in the basin

Non-uniform sediment compaction in sedimentary basins has also been documented (Debnath and Choudhuri 2010) presumably due to different compaction coefficient (defined in Appendix 1) of even the same sediment type (Dutta 1986), or due to the heterolithic sediments present (e.g., Galloway et al. 2009 and especially; Bjervik 2012). The uneven compression can be favoured by preferential accumulation of denser sediment at some part of the basin (Watts 2007).

Consider the dimension of the basin to be the same as the previous case but undergoing 'x' and 'y' rates of compression at its two margins (Fig. 1b). Up to Eq. (13) above, we proceed in the same way. In this case, the volume of the sediment after time 't' is

$$V = \left[h_0 - 0.5t(x+y) \right] l_0 b_0 = \left[V_0 - 0.5(x+y) l_0 b_0 t \right]. \tag{21}$$

Eliminating V from Eqs. (13) and (21)

$$\Delta T_2 = T - T_0 = \beta^{-1} \ln \left\{ 1 - 0.5(x+y) \beta l_0 b_0 t (V_0 \beta - knC_p)^{-1} \right\}. \tag{22}$$

Note $0.5(x+y)$ is the average rate of compression, say $= v'$. This average rate is attained at the middle of the compressing sediment layer.

Thus

$$\Delta T_2 = \beta^{-1} \ln \left\{ 1 - v' \beta l_0 b_0 t (V_0 \beta - krmC_p)^{-1} \right\}. \tag{23}$$

Eliminating 'm' from Eqs. (16) and (23)

$$\Delta T_2 = \beta^{-1} \ln \left\{ 1 - v' \beta l_0 b_0 t V_0^{-1} (\beta - kr\rho C_p)^{-1} \right\}. \tag{24}$$

Using the same arguments as that preceded Eq. (20), Eq. (24) is recast:

$$\Delta T_2 = \beta^{-1} \ln \left\{ 1 + \beta l_0 b_0 v' t V_0^{-1} (kr\rho C_p - \beta)^{-1} \right\}. \tag{25}$$

Obviously, 'v″ for uneven compression case in Eq. (26) is equivalent to 'v' for the uniform compression case in Eq. (20); so far, ΔT_1 and ΔT_2 are concerned. In addition, note, for a uniform compression case of $x=y=v$, Eq. (20) reduces to as Eq. (25). In addition, for $t=0$ in Eqs. (20) and (25), $\Delta T_1 = \Delta T_2 = 0$, which is as expected.

Conclusions and discussion

Considering clastic sedimentary mass as a single fluid in this work is the first-order approximation, which has been done by some of the previous authors in different tectonic contexts (e.g., Bruthanset al. 2006; Weinberger et al. 2006; Mukherjee et al. 2010; Mukherjee 2011). The actual physical behaviour of sediments under compression is available in Anandarajah and Lavoie (2002). Jones and Addis (1985) compared model-generated compression behaviour with the real behaviour of sediments. Protracted sediment compression can reduce porosity substantially and increase significantly pore pressure, and eventually, the yield strength of sediments reduces, since it is already strained. With increasing overburden pressure, average grain contacts per grain increases, also grains can crush due to the high fluid pressure developed. However, to the knowledge of the authors of this article, the heat produced due to such an event has not yet been constrained. As per Eqs. (20) and (25), temperature rise by compression of sediments in basins are functions of initial temperature of sediments, compression rate(s) for uniform (or non-uniform) compression, coefficient of volume expansion, isothermal compressibility, dimension (length, width, and depth), and density of sedimentary column and specific heat at constant pressure. However, the temperature rises by even and uneven compression, as per Eqs. (20) and (25), respectively, is not simply proportional to any of these parameters.

Density of rock column can vary in three directions: two perpendicular directions on the surface and the third vertically down the depth. Such a variation pattern of density may be known for the sedimentary basin, ideally before the compression started. In that case, Eqs. (20) and (25) are to be modified by involving the "effective density" terms that also includes wet bulk density (ρ_{bw}) of the sediment, matrix/mineral grain density (ρ_m), fluid density (ρ_f), depth (z), porosity at surface ($\emptyset_0$), and compaction constant (λ) as per Appendix 2. Basin subsidence rate, constrained from top surface, can be rapid: 0.02 cm $year^{-1}$, or it can be slow: 0.003 cm $year^{-1}$ (Watts and Ryan 1976; Clevis et al. 2003). Stanley and Corwin (2013) referred 0.37–0.84 cm $year^{-1}$, and Meckel et al. (2006) 0.5 cm $year^{-1}$. Usually, a higher sedimentation rate promotes a greater rate of compaction. The Red sea rift basin is ~1700 km long (Michon and Merle 2003).The South Caspian basin hosts the thickest sedimentary pile of 28 km (Knapp et al. 2007) known on the Earth. The molar mass (m), the coefficient of volume expansion (β), specific heat at constant pressure (C_p) within 25–500 °C, and density (ρ) for quartz are 60.08 gm $mole^{-1}$, 1.50×10^{-6}/°C, 10.63–17.11 Cal mol^{-1} K^{-1}, and 2.54 gm cm^{-3}, respectively. Note for rocks $\beta = 3\times10^{-5}$ (Stuwe 2007). For other sediment types, *"k"* can be ~6×10^{-10} Pa^{-1} (Parson et al. 2010) and C_p 1 kJ $kg^{-1}K^{-1}$ (De Lapp and Le Bouef 2004). Compressibility (isothermal) of sediments (k) is ~2.55×10^{-11} Pa^{-1} (Turgut 1997). Dandekar (2006), however, provided a different range (3×10^{-6} to 25×10^{-6} psi) for sediments. Compressibility of unconsolidated and consolidated sands and clays ranges 10^{-3} to 10^{-7} psi. For some particular clays, it ranges 5×10^{-4} to 2.9×10^{-5} psi (Chilingarian et al. 1995).

Considering rectangular parallelepiped-shaped sand layer of initial dimension 10 km (length) × 4 km (width) × 4 km (depth) consisting of quartz grains alone (~the case of quartz-dominated diagenesis, leading, therefore, to sedimentary quartzite: Allen and Allen 2013), for a spatially and temporally uniform compression rate of 0.37 cm $year^{-1}$, the temperature rise (ΔT_1) until 10^3 years is presented in Fig. 2. For modeling purpose, we impose the compressible fluid rheology on sand grains. A similar approach has been routinely adopted in geodynamics and structural geological modeling, where ductilely deforming rocks are equated with flowing fluids (Ramsay and Lisle 2000). The figure considers $C_P = 1.50\times10^{-6}$/°C, $k = 2.55\times10^{-11}$ Pa^{-1}, $\rho = 2.54$ gm cm^{-3}, $r = 0.017$ (because 1 mol of SiO_2 is equivalent to its mass of 60.08 g). Two points are to be noted. First, sediments must have a limit up to which they can compact after which they become material with relatively low compressibility. Second, pore fluid expelled during compaction would flush out the heat produced. Therefore, a non-stop temperature rise, as presented in Fig. 2, would not be possible in nature. Note that, for such chosen parameters, $V_0\beta = 24\times10^{10}$, which is $>>$ krmC_p = 0.73×10^4, so that ($V_0\beta$ − krmC_p) effectively equals $V_0\beta$. Thus, recollecting $V_0 = l_0 b_0 h_0$, Eqs. (20) and (25) simplified to

$$\Delta T_1 = \beta^{-1}\ln\left\{1 + vth_0{}^{-1}\right\}, \tag{27}$$

$$\Delta T_2 = \beta^{-1}\ln\left\{1 + v'th_0{}^{-1}\right\}. \tag{28}$$

This work considered a continuously acting pressure over the sediment layer. However, there are reports of temporal reduction of pressure on deep-sea marine sediments in some cases [review in Buchan and Smith (1999)], and the present model would not work in such cases.

Presenting the physical properties of matrix, void space and fluids together as a single parameter is sometimes done in basin analysis. For example, the "bulk compressibility" can be expressed as [as referred in Dandekar (2006)]

$$\mathrm{Cb} \approx (\partial\Phi/\partial P)T. \tag{29}$$

Few natural cases and processes were not considered in this model. These are (1) sediments dissolve and precipitate in deeper part of the basin, i.e., at > 2–3 km depth and at 70–100 °C (Bjorlykke 1999). Besides carbonates, density of newly deposited sediments ranging 1.6–1.9 gm cm^{-3} increase to ~2.6–2.8 gm cm^{-3} (Lerche and Patersen 1995). In this process, sediment strength also elevates from 5×10^6 to 5×10^8 psi (Lerche and Patersen 1995). Potter et al. (2005), therefore, rightly stated "…compaction is more than just physical compression…". (2) The thermal conductivity of the basement and the sediments above it can be 3.4 and 2.5 $Wm^{-1}K^{-1}$ (Armstrong and Chapman 1999), although thermal conductivities of sediments in basins are not well known (Blackwell and Steele 1989). As sediments compact, thermal conductivity presumably increases (Tari et al. 1999). Furthermore, interstitial water, depending on the cation exchange capacity and the salinity, can have a much higher thermal conductivity than ordinary water in the lab (Drost-Hansen 1991). (3) The modeled situation of temperature rise can get complicated, since basins can also subside as a whole. (4) Two sets of faulting could be produced in real sedimentary bodies for the kind of compression envisaged here if prolonged (Lonerganet al. 2002). (5) Allen and Allen (2013) distinguished three interlinked processes, while sediments compact: (i) compressibility: of sediments; (ii) compaction: of pore space; and (iii) consolidation: water expels. These details are not explored in this work. (6) The basin geometry can commonly be a synclinal structure

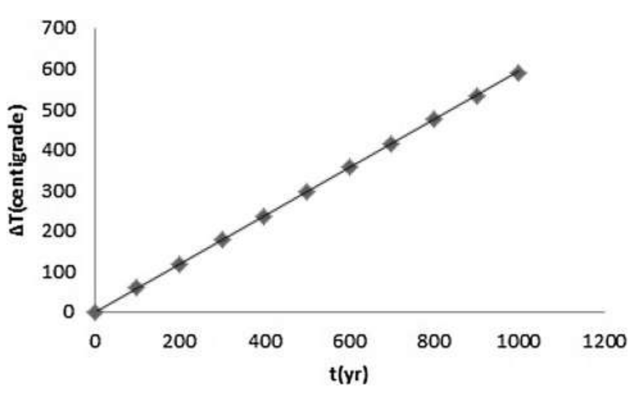

Fig. 2 Temperature rise by uniform compression of sediments, see "Conclusions and discussion" for the parameters chosen

(Chakraborty et al. 2003). (7) Pore fluid and sediments can have different thermal–mechanical properties. For example, compressibility (and density) of the pore fluid can be ~10 times higher (and less than half) than that of the sediment (Table 1 of Turgut 1997). To our knowledge, nobody yet modeled temperature rise for compacting sediments considering all these constraints presumably because the model then complicates. (8) Exchange of heat is likely between pore-filling fluid and the porous matrix. Second, the thermal conductivity decreases as porosity increases (Jackson and Richardson 2007).

Clay converts from one variety to another at ~70–90 °C (Woden and Burley 2003), at 2–3 km burial depth (Allen and Allen 2013). This is close to the range of burial diagenetic temperature of 80–100 °C (Hansley and Whitney 1990). Significant dehydration from clays takes place at ~105 °C (Weaver et al. 1971). The highest diagenetic temperature can be ~120 °C (Lin et al. 2017), or probably 170 °C (Renchao et al. 2012). The present work indicates that diagenetic temperature may not be simply depth-controlled, and compression-related temperature should contribute to heating and possibly augment in diagenesis as well. Diagenesis at shallow depth such as merely 10 m as reported by Huggett et al. (2017) from mudrocks in Jordan may be attributed to such a compression-related temperature rise. As per the chosen parameters, 70–120 °C temperature rise can arise within ~150 years (vide Fig. 2). Since clay and mud compress more easily, one can expect temperature rise to be more pronounced in these sediments when they lithify.

Acknowledgements Research sabbatical for the year 2017 and the CPDA grant received from IIT Bombay supported SM. Editorial handling by Christian Dullo, Monika Dullo and the Topic Editor. Detail review by an anonymous reviewer.

Appendix 1

The compaction coefficient/uniaxial compressibility is (Fjar et al. 2008)

$$\Delta h/h = C_m \alpha \Delta P_f, \tag{29}$$

where Δh is the change in height of sedimentary layer due to compaction, h is the initial height of the layer, C_m is the coefficient of uniaxial compression, α is the Biot's poro-elastic parameter, and ΔP_f is the change in pore fluid pressure.

Appendix 2

As per Mukherjee (2017; also see Mukherjee 2018a, b, c for similar equations), k_x is the density gradient along X-horizontal direction up to a distance l_0 and k_y is the density gradient along a perpendicular Y direction up to a distance b_0. Vertically down along Z direction, and up to h_0 distance porosity falls as per Athy's exponential law. In this case,

$$\rho_e = \rho_m + 0.5\left(k_x l_0 + k_y b_0\right) + \left(\rho_m - \rho_f\right)\emptyset_0 {z_1}^{-1} \lambda\left(\exp^{-ho}\lambda^{-1} - 1\right). \tag{30}$$

Symbols defined in "Conclusions and discussion". ρ_e can be substituted in place of ρ in Eqs. (20) and (26) and proceeded for the subsequent derivations.

References

Allen PA, Allen JR (2013) Basin analysis: principles and applications to petroleum play assessment. 3rd edn. Wiley Blackwell, Hoboken, p 327

Anandarajah A, Lavoie D (2002) Numerical simulation of the microstructure and compression behavior of Eckernförde Bay sediments. Mar Geol 182:3–27

Armstrong PA, Chapman DS (1999) Combining tectonics and thermal fields in Taranaki Basin, New Zealand. In: Forster A, Merriam DF (eds) Geothermics in basin analysis. Springer Science + Business Media LLC, Berlin, pp 151–176

Bjervik AS (2012) Seimic analysis of Carboniferous rift basin and Triassic growth-fault basins of Svalbard; analysis of seismic facies patterns with bearing on basin geometry and growth-strata successions. Thesis. Norwegian University of Science and Technology, pp 1–99

Bjorlykke K (1999) Principal aspects of compaction and fluid flow in mudstones. In: Aplin AC, Fleet AJ, Macquaker JHG (Eds) Muds and mudstones: physical and fluid flow properties. Geological Society London Special Publications, London, vol 158, pp 73–78

Blackwell DD, Steele JL (1989) Thermal conductivity of sedimentary rocks: measurement and significance. In: Naeser ND, McCulloh TH (eds) Thermal history of sedimentary basins. Springer, New York, pp 13–35

Blatt H, Middleton G, Murrey R (1972) Origin of sedimentary rocks. 2nd edn. Prentice-Hall, New Jersey, p 192

Bruthans J, Fillipi M, Gersl M, Zare M, Melkova J, Pazdur A, Bosak P (2006) Holocene marine terraces on two salt diapirs in the Persian Gulf, Iran: age, depositional history and uplift rates. J Quarter Sci 21:843–857

Buchan S, Smith DT (1999) Deep-Sea sediment compression curves: some controlling factors, spurious over-consolidation, predictions, and geophysical reproduction. Marine Geores Geotechnol 17:65–81

Chakraborty C, Mandal N, Ghosh SK (2003) Kinematics of the Gondwana basins of peninsular India. Tectonophysics 377:299–324

Chilingarian GV, Rieke HH, Donaldson EC (1995) Compaction of argillaceous sediments. In: Chilingarian GV, Donaldson EC, Yen TF (eds) Subsidence due to fluid withdrawal. Elsevier, Amsterdam, pp 47–164

Clevis Q, de Boer P, Wachter M (2003) Numerical modelling of drainage basin evolution and three-dimensional alluvial fan stratigraphy. Sediment Geol 163:85–110

Cloetingh S, Ziegler PA (2007) Tectonic models for the evolution of sedimentary basins. In: Watts AB (ed) Treatise on geophysics. Elsevier, Amsterdam, pp 486–611

Dandekar AY (2006) Petroleum Reservoir Rock and Fluid Properties, CRC Press, Boca Raton, pp 488

Debnath K, Chaudhuri S (2010) Bridge pier scour in clay-sand mixed sediments at near-threshold velocity for sand. J Hydraulic Eng 136:597–609

De Lapp RC, Le Boeuf EJ (2004) Thermal analysis of whole soils and sediment. J Environ Qual 33:330–337
Drost-Hansen W (1991) Some effects of vicinal water on the sedimentation process, compaction, and ultimate properties of sediments. In: Bennett RH, Bryant WR, Hulbart MH (eds) Microstructures of fine-grained sediments: from mud to shale. Springer, New York, p 264
Dutta NC (1986) Shale compaction, burial diagenesis, and geopressures: a dynamic model, solution and some results. In: Burrus J (ed) Thermal modeling in sedimentary basins. Gulf Publishing Company, Houston, pp 149–172
Fjar E, Holt RM, Raaen AM, Risnes R, Horsrud P (2008) Petroleum related rocks mechanics. 2nd edn. Elsevier, Amsterdam, p 393
Galloway WE, Ganey-Curry P, Whiteaker TL (2009) Regional controls from temporal and spatial distribution of continental slope and Abyssal Plain Reservoir Systems of the Gulf of Mexico Basin. Search and Discovery Article #50226. AAPG Database
Hansley PL, Whitney CG (1990) Petrology, Diagenesis, and Sedimentology of Oil Reservoirs in Upper Cretaceous Shannon Sandstone Beds, Powder River Basin, Wyoming. US Geol Surv Bull
Hantschel T, Kauerauf AI (2008) Fundamentals of basin and petroleum system modeling. pp 31–101
Huggett J, Hooker JN, Cartwright J (2017) Very early diagenesis in a calcareous, organic-rich mudrock from Jordan. Arab J Geosci 10:270
Jackson D, Richardson M (2007) High-frequency seafloor acoustics. Springer, Berlin (**ISBN 978-0-387-34154-5**)
Jones ME, Addis MA (1985) On changes in porosity and volume during burial of argillaceous sediments. Mar Pet Geol 2:247–253
Knapp JH, Knapp CCD, Connor JA, McBride JH, Simmons MD (2007) Deep seismic exploration of the South Caspian Basin: lithospherescale imaging of the world's deepest basin. In: Yilmaz PO, Isaksen GH (Eds) Oil and gas of the Greater Caspian area. AAPG Studies in Geol, vol 55, pp 47–49
L'Heureux I, Fowler AD (2000) A simple model of flow patterns in overpressured sedimentary basins with heat transport and fracturing. J Geophys Res 105:23741–23752
Lerche I, Petersen K (1995) Salt and sediment dynamics. CRC Press, Boca Raton, pp 1–4
Lin W, Chen L, Lu Y, Hu H, Liu L, Liu X, Wei W (2017) Diagenesis and its impact on reservoir quality for the Chang 8 oil group tight sandstone of the Yanchang formation (upper Triassic) in southwestern Ordos basin, China. J Petrol Expl Prod Tech 7:947–959
Lonergan L, Cartwright J, Laver R, Staffurth J (2002) Polygonal faulting in the Tertiary of the central North Sea: implications for reservoir geology. In: Holdsworth RH, Turner JP (eds) Extensional tectonics: faulting and related processes. The Geol. Soc., Key Issues in Earth Sciences, vol 2, pp 299–315
Meckel TA, ten Brink US, Williams J (2006) Current subsidence rates due to compaction of Holocene sediments in southern Louisiana. Geophys Res Lett 33:L11403
Michon L, Merle O (2003) Mode of lithospheric extension: Conceptual models from analogue modeling. Tectonics 22:1028
Mukherjee S (2011) Estimating the viscosity of rock bodies—a comparison Between the Hormuz- and the Namakdan Salt Domes in the Persian Gulf, and the Tso Morari Gneiss Dome in the Himalaya. J Ind Geophys Union 15:161–170
Mukherjee S (2017) Airy's isostatic model: a proposal for a realistic case. Arabian J Geosci 10:268
Mukherjee S (2018a) Locating center of pressure in 2D geological situations. J Ind Geophys Union 22:49–51
Mukherjee S (2018b) Locating center of gravity in geological contexts. Int J Earth Sci 107:1935–1939
Mukherjee S (2018c) Moment of inertial for rock blocks subject to bookshelf faulting with geologically plausible density distributions. J Earth Sys Sci. https://doi.org/10.1007/s12040-018-0978-4
Mukherjee S, Talbot CJ, Koyi HA (2010) Viscosity estimates of salt in the Hormuz and Namakdan salt diapirs, Persian Gulf. Geol Mag 147:497–507
Murton BJ, Biggs J (2003) Numerical modelling of mud volcanoes and their flows using constraints from the Gulf of Cadiz. Marine Geol 195:223–236
Nemec W (1988) Coal correlations and intrabasinal subsidence: a new analytical perspective. In: Kleinspeheu KL, Paola C (eds) New perspectives in basin analysis. Springer, New York, pp 161–188
Parson M, Banerjee A, Rupp J, Medina C, Lichtner P, Gable C, Pawar R, Celia M. McIntosh J, Bense V (2010) Assessment of basin-scale hydrologic impacts of CO_2 sequestration, Illinois basin. Int J Greenhouse Gas Control 4:840–854
Payne FC, Quinner JA, Potter ST (2008) Remediation hydraulics. CRC Press, Boca Raton, p 40
Pettijohn FJ (2004) Sedimentary rocks, 3rd edn. CBS Publishers and Distributors, New Delhi, pp 276
Potter PE, Maynard JB, Depetris PJ (2005) Mud and mudstones: introduction and overview, pp. 129. Springer, Berlin, p 130
Ramsay JG, Lisle R (2000) The Techniques of modern structural geology: applications of continuum mechanics in structural geology, vol 3. Academic Press, San Francisco, p 926
Renchao Y, Aiping F, Zuozhen H, Xiuping W (2012) Diagenesis and porosity evolution of sandstone reservoirs in the East II part of Sulige gas field, Ordos Basin. Int J Mining Sci Tech 22:311–316
Rieke HH, Chilingarian GV (1974) Compaction of argillaceous sediments. Elsevier Scientific Publishing Company, Amsterdam, pp 1–424
Ryer TA, Langer AW (1980) Thickness change involved in the peat-to-coal transformation for a bituminous coal of Cretaceous age in central Utah. J Sedi Res 50:987–992
Stanley J-D, Corwin KA (2013) Measuring strata thicknesses in cores to assess recent sediment compaction and subsidence of Egypt's Nile delta coastal margin. J Coastal Res 29:657–670
Stuwe K (2007) Geodynamics of the lithosphere. 2nd edn, Springer, Berlin, p 272
Tari G, Dovenyi P, Dunkl I, Horvath F, Lenkey L, Stefannescu M, Zafian PS, Toth T (1999) Lithosphric structure of the Pannonian basin derived from seismic, gravity and geothermal data. In: Durand B, Jolivet L, Harvath F, Serranne M (eds) The Mediterranean basins: tertiary extension within the Alpine Orogen. Geological Society London Special Publications, London, vol 156, pp 215–250
Tucker M (1981) Sedimentary petrology: an introduction. Blackwell Scientific Publications, Hoboken, p 87
Turgut A (1997) Inversion of bottom/subbottom statistical parameters from acoustic backscatter data. J Acoustical Soc Am 102:833–852
Wangen M (2010) Physical principles of sedimentary basin analysis. Cambridge University Press, Cambridge
Watts AB (2007) Lithospheric flexure due to prograding sediment loads: implications for the origin of offlap/onlap patterns in sedimentary basins. Basin Res 2:133–144
Watts AB, Ryan WBF (1976) Flexure of the lithosphere and continental margin basins. Tectonophysics 36:25–44
Weaver CE, Beck KC, Pollard CO (1971) Clay Water diagenesis during burial: how mud becomes gneiss. Geol. Soc. Am. Spec. Pap., p 134, https://doi.org/10.1130/SPE134-p1
Weeks LG (1952) Factors of sedimentary basin development that control oil occurrence. AAPG Bull 36:2071–2124
Weinberger R, Lyakhovsky V, Baer G, Begin ZB (2006) Mechanical modeling and InSAR measurements of Mount Sedom uplift, Dead Sea basin: Implications for effective viscosity of rock salt. Geophys Geochem Geosys 7Q:05014
Wood RJ (1981) The subsidence history of Conoco well 15/30-1, central North Sea. Earth Planet Sci Lett 54:306–312
Worden RH, Burley S (2003) Sandstone diagenesis: the evolution of sand to stone. In: Burley S, Worden RH (eds) Sandstone diagenesis: recent and ancient. Blackwell Publishing, Hoboken, pp 3–44